Int. J. Heat Mass Transfer. Vol. 33, No. 4, pp. 649–659, 1990
Printed in Great Britain

0017–9310/90 $3.00 + 0.00

An experimental investigation of the reversibility and hysteresis of the condensation curves

YOSHIO UTAKA and AKIO SAITO
Department of Mechanical Engineering, Tokyo Institute of Technology, 2-12-1 Ookayama, Meguro-ku, Tokyo 152, Japan

and

HIROYUKI YANAGIDA
Kao Co., 2606 Akabane, Ichigai-cho, Haga-gun, Tochigi 321-34, Japan

(*Received* 29 *November* 1988 *and in final form* 23 *June* 1989)

Abstract—An experimental study is performed on the transition characteristics concerning the reversibility and the hysteresis loop of the condensation curve. From the results of condensation experiments using propylene glycol vapor on lyophobic surfaces, having three different edge conditions of wettable, partially non-wettable and non-wettable, it is proved that the transition modes are greatly affected by these conditions. Under a large overall cooling-side conductance which realizes the continuous curve during the process of increasing surface subcooling, the reversible and/or hysteresis curves are obtained. The transition modes during the process of decreasing subcooling are closely related to the aspects of condensation in increasing subcooling. Although the modes for increasing subcooling are determined by the instability of the overall heat transfer system, they are strongly influenced by the edge conditions and the vapor force as well. Under a small overall cooling-side conductance which brings about the jump mode, the hysteresis loops appear in all cases.

1. INTRODUCTION

THE CHARACTERISTICS of a condensation curve, which show the change of the heat flux against the surface subcooling, have not yet been investigated thoroughly. A study is made in this paper on the transition mode concerning the reversibility and the hysteresis in which the curves obtained by decreasing and increasing surface subcoolings follow different routes. For the case of increasing subcooling, the measurements of condensation curves have been performed for several kinds of vapors, i.e. steam [1–3], aniline, nitrobenzene [4], ethylene glycol [5, 7], propylene glycol [6–8], and glycerol [7]. In general, when the subcooling of a lyophobic condensing surface is increased slowly enough to keep a quasi-steady state during the condensation of vapor, the heat flux reaches its maximum value and then decreases gradually. With a further increase of subcooling, after the aspect of condensation shifts from dropwise to film mode near the point of minimum heat flux (MHF), the heat flux increases in the region of the film mode. The transition mode here can be classified into two types, i.e. continuous and jump transitions. In a previous paper [8] the heat transfer mechanism determining the transition mode from dropwise to film condensation was discussed theoretically and experimentally. It was proved that the jump occurs in the negative gradient domain of the condensation curve and is determined by the instability of the overall heat transfer system. The factors controlling the phenomena are the gradient of the condensation curve on the bilogarithmic coordinates and the ratio of the condensation heat transfer coefficient to the overall cooling-side conductance (the overall thermal conductance per unit area between the condensing surface and the coolant). Even in the case where a discontinuous jump occurs on the condensation curve, the curve can be made continuous by increasing only the overall cooling-side conductance.

The condensation curves seem to follow hysteresis loops. In case a hysteresis loop exists, there is a region in which the mode of condensation depends on the initial condition or the history of the process. Therefore, it is important to clarify how the mode shifts from the film mode to the dropwise mode under a given condition. Although a considerable amount of research has been carried out for the process of increasing surface subcooling as mentioned above, few studies are available for decreasing surface subcooling. In the experiments of Takeyama and Shimizu [1] and Izumi *et al.* [3], so-called hysteresis loops were observed. However, their experimental conditions were not clearly specified because the edges of heat transfer blocks, usually utilized in the experiments, might have broken the condensate film. Further, the experiments were made only under a small overall cooling-side conductance, causing jump transitions, especially in ref. [3]. Since a liquid film is relatively stable during condensation of vapor, the edge condition, in addition to the instability of the overall heat transfer system, will have an important role in

NOMENCLATURE

C	overall cooling-side conductance [kW m^{-2} K^{-1}]	Greek symbol	
m	vapor mass velocity [kg m^{-2} s^{-1}]	τ	time [s].
q	heat flux [kW m^{-2}]	Subscripts	
T	temperature [K]	c	coolant
ΔT	degree of condensing surface subcooling [K]	min	minimum heat flux point
t	time from the jump start [s].	v	vapor saturation
		l	thermocouple nearest to the condensing surface.

determining the transition mode from film to dropwise condensation.

The objective of this study is to investigate the mode of transition from film to dropwise condensation, with specified edge conditions of the condensing surface. In particular, the difference between the condensation curves for increasing and decreasing surface subcoolings and the relation between such a difference and the aspects of the condensate on the condensing surface are clarified. Also the criteria realizing the reversible change without a hysteresis loop are determined.

2. EXPERIMENTAL APPARATUS AND METHOD

The schematic of the experimental apparatus is shown in Fig. 1. Since the procedure was similar to the one presented in previous papers [6, 7], only the main and modified items will be highlighted here. The vapor generator (30L) and the condenser capacity were made large, about five times the former one in order to increase the flow rate of the vapor. The pressure and the flow rate of the vapor passing through the condensing chamber could be kept constant at prescribed values by adjusting the pressure control valve with vacuum suction of the container placed next to the condenser. The condensate was returned continuously by gravity through the return tube. Hence, the condensate return valve was always open.

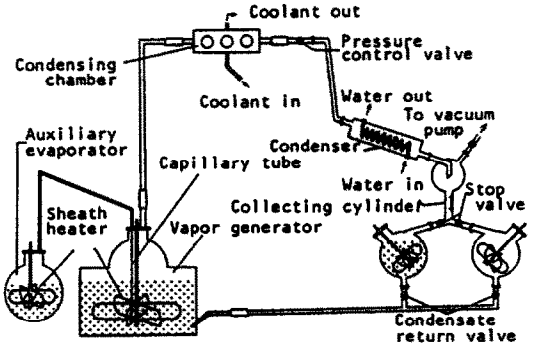

FIG. 1. Experimental apparatus.

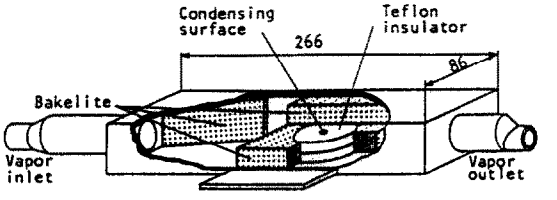

FIG. 2. Condensing chamber.

Figure 2 illustrates the condensing chamber. The heat transfer block was mounted at the center of it. The vapor passage (18 mm × 18 mm) was relatively large to ensure enough rate of vapor flow. The propylene glycol and trilauryl trithiophosphite [$(C_{12}H_{25}S)_3P$] were used as a test vapor and a promoter for dropwise condensation, respectively. Figure 3 shows the cooling chamber attached behind the condensing chamber. The coolant jet impinged upon the bottom of the heat transfer block. Water, oil and ethylene glycol were used as the coolants to change the cooling intensity.

The condensing block made of copper is illustrated in Fig. 4. The size of the condensing surface was the same as the previous study (8 mm diameter). The thickness of the block was reduced to widen the adjustable range of the overall cooling-side conductance. A circular groove was cut and was filled with silicone resin insulator so that the heat flux and

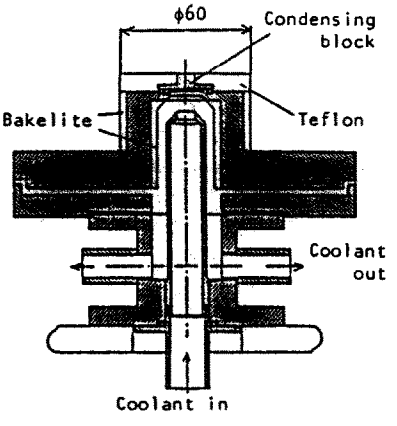

FIG. 3. Cooling chamber.

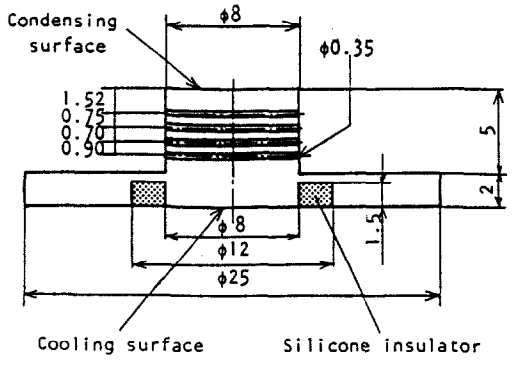

FIG. 4. Details of condensing block.

the surface temperature could be determined by assuming one-dimensional conduction. Four holes of 0.35 mm in diameter were drilled parallel to the condensing surface. The constantan wires of 0.1 mm in diameter, which were fixed in the thin glass tubes for fixing the location and for electrical insulation, were soldered at the center of each hole. The rest of the holes were filled with solder. A copper wire was soldered at the root of the copper block. The heat flux and the surface temperature were determined from the e.m.f.s of those thermocouples and their distances from the condensing surface.

Considering that the transition modes are likely controlled by the edge conditions, three condensing surfaces (called hereafter heat transfer surfaces I, II and III) were prepared as shown in Fig. 5. The heat transfer block shown in Fig. 4 was commonly used for these edge conditions. The vapor flowed from left to right for all the heat transfer surfaces. Each surface had characteristics as follows.

Heat transfer surface I (wettable edge). The side surface of the block up to an axial distance of 1 mm from the condensing surface was electroplated with chromium 0.1 mm thick. The whole surface was finished as shown in Fig. 5(a). Since the promoter of trilauryl trithiophosphite was not adsorbed to chromium, a thin wettable edge was realized perfectly over the whole periphery.

Heat transfer surface II (partially non-wettable edge). An alloy of bismuth and tin having a very low thermal conductivity was soldered partially at the side edge of the block. It was placed on the upstream side of the condensate flow. The whole surface was electroplated with copper as illustrated in Fig. 5(b).

Heat transfer surface III (non-wettable edge). The same alloy as used for heat transfer surface II was soldered over the whole periphery of the condensing surface except the portion around the downstream side of the condensate flow. Then the whole surface was electroplated with copper.

Here, for heat transfer surfaces II and III, the copper surfaces on the alloy of bismuth and tin had the same non-wettability as that of the condensing surface. However, the surface on the additional alloy having low thermal conductivity maintained a higher temperature due to a fin effect. Hence, dropwise condensation remained and the surfaces acted as non-wettable areas even when the subcooling of the main part of the condensing surface was very large.

The method of quasi-steady continuous measurement was utilized; that is, the coolant temperature increases or decreases very slowly, keeping the pumping power of the coolant constant. In this way, the start and end points of the jump were easily distinguished. Further, the measurements of both processes of increasing and decreasing surface subcoolings were performed consecutively to keep immutable states of the vapor and the heat transfer surface. The aspect of condensation was video-recorded simultaneously.

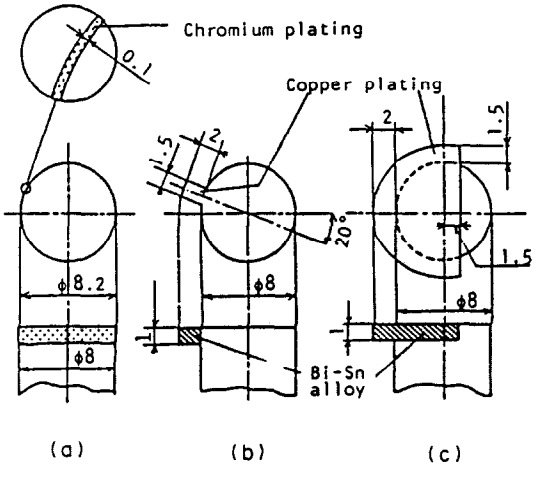

FIG. 5. Details of heat transfer surface: (a) heat transfer surface I; (b) heat transfer surface II; (c) heat transfer surface III.

3. RESULTS

The two vapor conditions (vapor conditions 1 and 2) shown in Table 1 were selected commonly for each of the heat transfer surfaces. T_v and m denote the saturation temperature and the vapor mass velocity, respectively. From the measurements in the former reports, the difference in the saturation temperature of the two vapor conditions was confirmed to have little effect on the aspect of condensation. The vapor force acting on the condensate was smaller under vapor condition 1 and larger under vapor condition

Table 1. Vapor conditions

Vapor condition	T_v (K)	m (kg m^{-2} s^{-1})
1	353	0.53
2	348	0.80

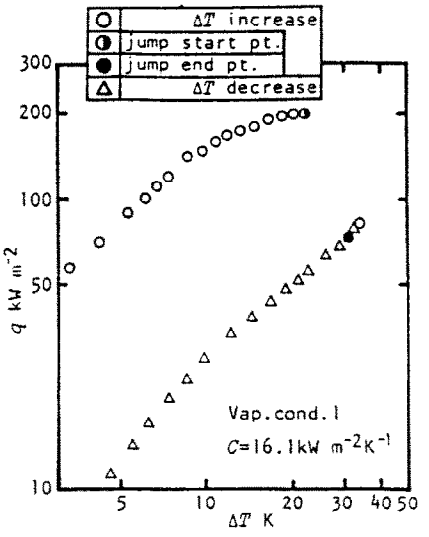

FIG. 6. Condensation curve using heat transfer surface I under vapor condition 1.

2. The measurements were also carried out for various overall cooling-side conductances.

3.1. *Wettable edge (heat transfer surface I)*

Figures 6 and 7(a) show the condensation curves using the heat transfer surface I for vapor conditions 1 and 2. The overall cooling-side conductance C was kept almost constant for both of the cases. The value was also kept constant for all condensation curves to be shown later. The circular and triangular symbols correspond to the processes of increasing and decreasing surface subcoolings, respectively. A jump was observed in the process of increasing surface subcooling. Dropwise condensation shifted abruptly to film condensation, which started near the maximum heat flux point. The start and end points of the jump are represented by half closed and closed symbols, respectively, in all the figures given hereafter. After the surface subcooling was increased further in the region of film condensation, the process was traced backwards

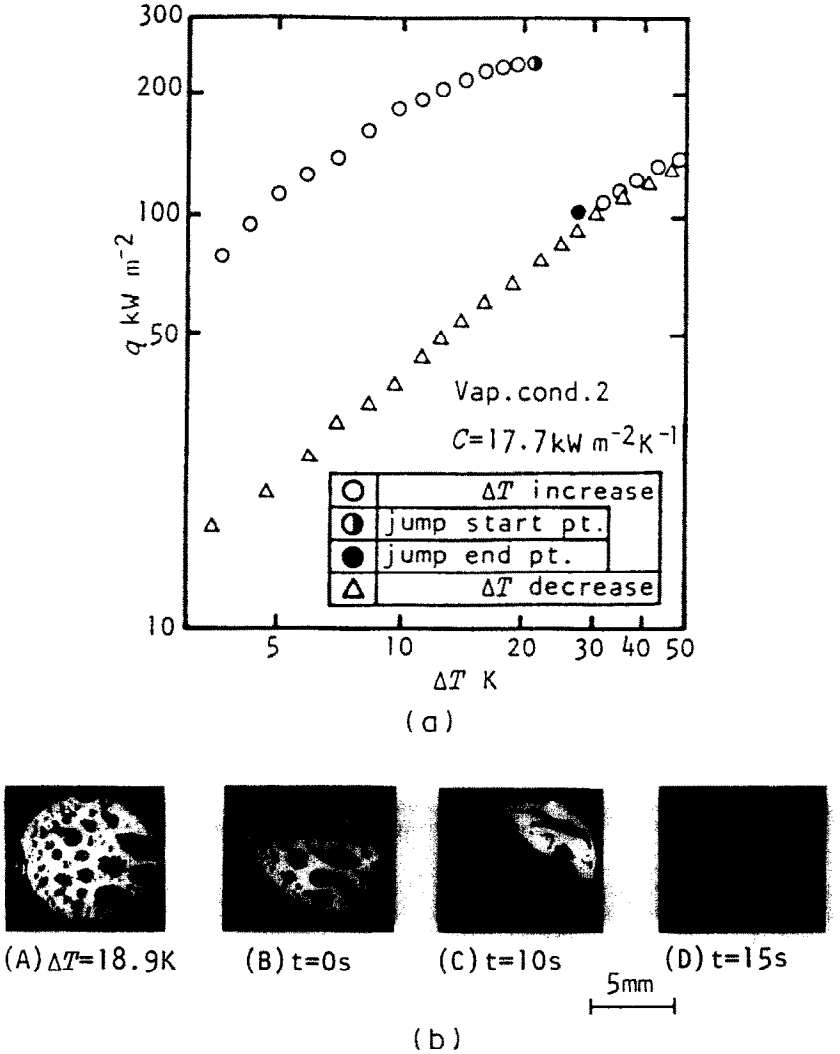

FIG. 7. Results using heat transfer surface I under vapor condition 2: (a) condensation curve; (b) aspects of condensation.

by decreasing the surface subcooling. Even when the surface subcooling was further decreased beyond the end point of the forward jump, the mode of condensation did not return to dropwise condensation. Film condensation remained until the surface dried up completely and the surface temperature became higher than the vapor saturation temperature. Thus, for the heat transfer surface I (wettable edge condition), large hysteresis loops were drawn independently of the vapor condition. Figure 7(b) shows photographs of the abrupt transition from dropwise to film condensation in the unsteady jump region of the curve given in Fig. 7(a). Here ΔT and t denote the surface subcooling and the time after the beginning of the jump, respectively. The vapor flow was from left to right and the gravitational force was in the downward direction.

3.2. *Partially non-wettable edge (heat transfer surface II), large overall cooling-side conductance*

Figures 8 and 9 show the results for the large overall cooling-side conductances obtained by using the heat transfer surface II with a partially non-wettable edge. Two different transition curves from film to

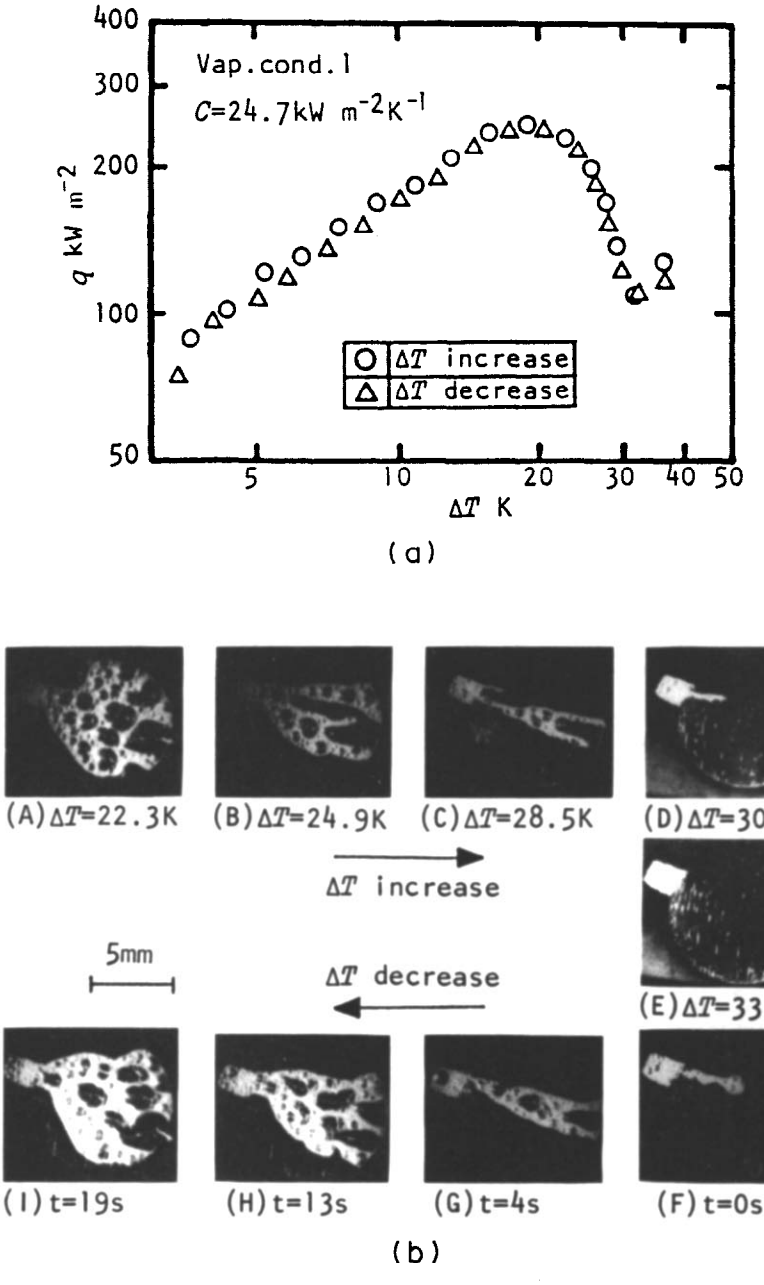

FIG. 8. Results using heat transfer surface II under vapor condition 1 : (a) condensation curve ; (b) aspects of condensation.

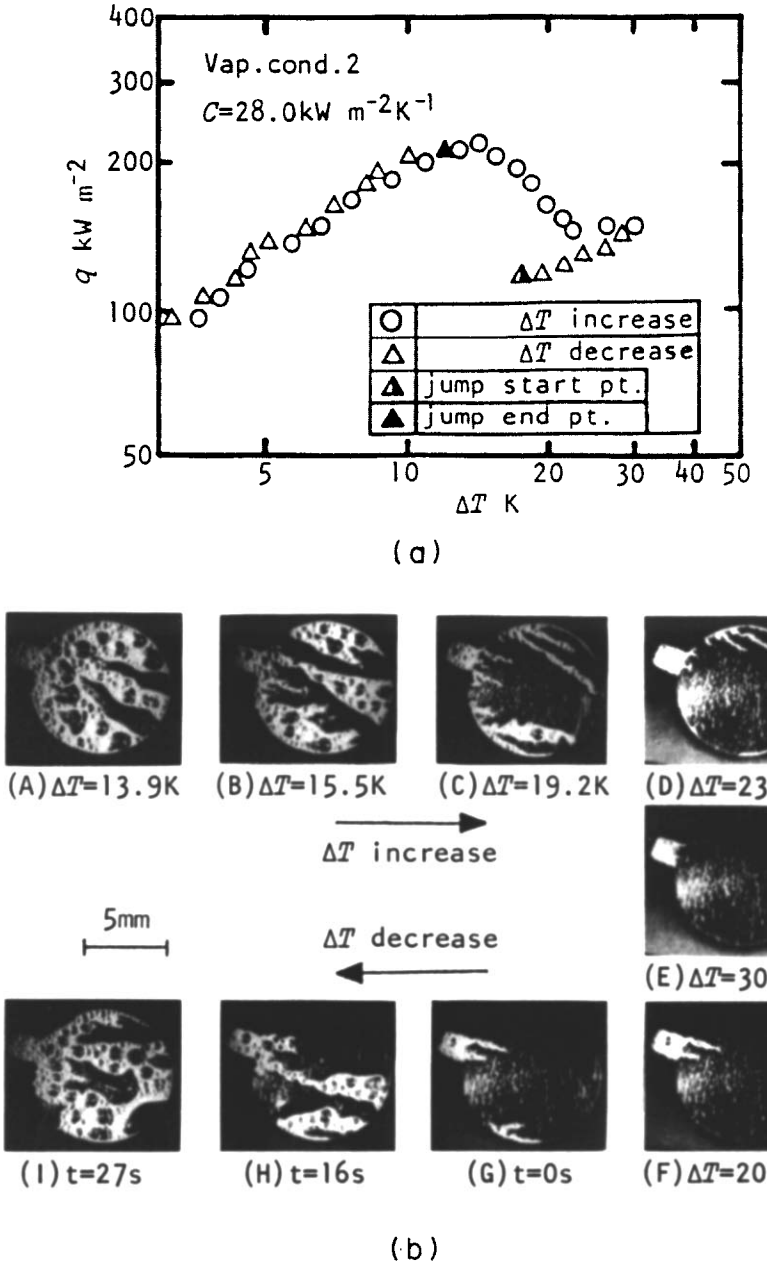

FIG. 9. Results using heat transfer surface II under vapor condition 2: (a) condensation curve; (b) aspects of condensation.

dropwise condensation were obtained. Figure 8(a) is the condensation curve for vapor condition 1. The reversible and continuous curve was obtained, i.e. the curve of increasing subcooling coincided with that of decreasing subcooling precisely. Figure 8(b) shows the variation of the aspects of condensation along the curve shown in Fig. 8(a). Photographs (A)–(E) are for the process of increasing subcooling and (E)–(I) are for the decreasing process. Since the photograph showing the aspect of condensation under decreasing subcooling was not taken, the case of the jump mode (photographs (F)–(I)) of the same vapor condition and of smaller overall cooling-side conductance is substituted here. The variation of the aspects of condensation was almost similar to that of the continuous mode. It is confirmed that the square part of the non-wettable region maintained the dropwise mode even when the remaining surface was entirely covered with condensate film. These photographs exhibit a kind of symmetrical nature between increasing and decreasing subcoolings with respect to photograph (E) of film condensation. This agrees with the trend of the condensation curves.

Figure 9(a) shows the condensation curve for vapor condition 2 of larger vapor force. The continuous curve was obtained for increasing subcooling, similar

to Fig. 8(a). However, the curve for decreasing subcooling was broken by a jump, even when the overall cooling-side conductance was the same as the one for increasing subcooling. In the film region from larger subcooling to the MHF point of increasing subcooling, the curves for decreasing and increasing subcoolings coincided with each other. Nevertheless, film condensation continued further at a certain subcooling smaller than that of the MHF point of increasing process. Then the jump to the dropwise mode occurred from the point indicated by a symbol Δ to the point ▲ in the figure. The curves for both processes agreed again in the dropwise region. Figure 9(b) shows the photographs of condensation of Fig. 9(a). Photographs (A)–(E) show the process of increasing subcooling and photographs (E)–(I) give the decreasing process showing the jump mode. In the decreasing process, the break of liquid film progressed not only from the non-wettable part but also from the lower edge of the condensing surface and was triggered by it as seen in photographs (G) and (H); that process was in contrast to the reversible curves in which the liquid film was broken only from the partially non-wettable edge shown in Fig. 8. Thus the aspects of condensation as well as the condensation curves showed irreversible changes under vapor condition 2.

3.3. *Non-wettable edge (heat transfer surface III), large overall cooling-side conductance*

The result of measurements using heat transfer surface III, the periphery of which is almost surrounded by the non-wettable material, is shown in Figs. 10 and 11. The overall cooling-side conductances were also large. Vapor condition 1 was employed. The results for increasing and decreasing subcoolings coincided. Figure 10(b) shows the variation of the aspects of condensation along the curves of Fig. 10(a). Photographs (A)–(E) and (E)–(I) are for the increasing and decreasing processes, respectively. It is also confirmed by these photographs that the surface area made of alloy of low thermal conductivity always kept the dropwise mode. Since those photographs show a symmetry with respect to photograph (E), the change of aspects of condensate was confirmed to be reversible. The condensation curves and the aspects of condensation under vapor condition 2 are also given in Figs. 11(a) and (b), respectively. They were the same as those for vapor condition 1. Thus, the continuous and reversible curves were always measured independently of the vapor condition for heat transfer surface III.

Figure 12 shows the variations of temperatures. It confirms the quasi-steady change of the coolant temperature T_c and the temperature T_1, which was measured by the thermocouple in the condensing block nearest to the condensing surface (about 1.5 mm beneath), while the vapor temperature T_v was kept constant.

Figure 13 illustrates schematically the transition modes when using heat transfer surfaces I–III under large overall cooling-side conductance to achieve the continuous mode during the process of increasing subcooling.

3.4. *Small overall cooling-side conductance*

The measurements of condensation curves with relatively small overall cooling-side conductances, which lead to the jump transitions, are described in the following. Figures 14(a) and (b) are the results under the same vapor conditions as those of Figs. 8(a) and 11(a), respectively, in which the reversible and continuous curves were obtained. The solid lines show those continuous curves. The jump modes for both increasing and decreasing surface subcoolings were obtained. Each datum except the unconnected jump region coincided quite well with the continuous curve. These jump phenomena for increasing subcooling should be determined by the instability of the overall heat transfer system [8]. However, since the temperature distribution in the condensing block was somewhat distorted from a one-dimensional conduction owing to the additional alloy at the edge, the quantitative discussion of the instability is withheld here. In the processes of increasing subcooling both for Figs. 14(a) and (b), each end point of the jump (●) shifted toward the region of surface subcooling larger than the one of the MHF points of the continuous mode. It occurred as a result of the reduction of overall cooling-side conductance under the same heat transfer surface and the same vapor condition. The reason for this is that the cooling intensity balancing theoretically to the continuous curve decreases along the curve with the increase of subcooling in the region of the negative gradient. As will be shown, the start points of the jump (Δ) from film to dropwise condensation coincided with the MHF points of the continuous curves. Therefore, the cooling intensity at the MHF point of decreasing subcooling is smaller than that at the end point of the jump of increasing subcooling. Since the cooling intensities at the start and end points of the jump are equal, the surface subcooling at the end point of the jump from film condensation is smaller than that at the start point of the jump from dropwise condensation. Hence, when the jump transition occurs for increasing subcooling due to the instability of the overall heat transfer system, the condensation curve has a hysteresis loop.

4. DISCUSSION

On the basis of the results described above, the difference in the modes of film-to-dropwise transition is discussed here. When the curves for increasing and decreasing surface subcoolings coincided (Figs. 8(a), 10(a) and 11(a)), the aspects of condensate on the condensing surface showed symmetrical and reversible change as shown in Figs. 8(b), 10(b) and 11(b). On the other hand, both of the condensation curves and the aspects of condensation show unsym-

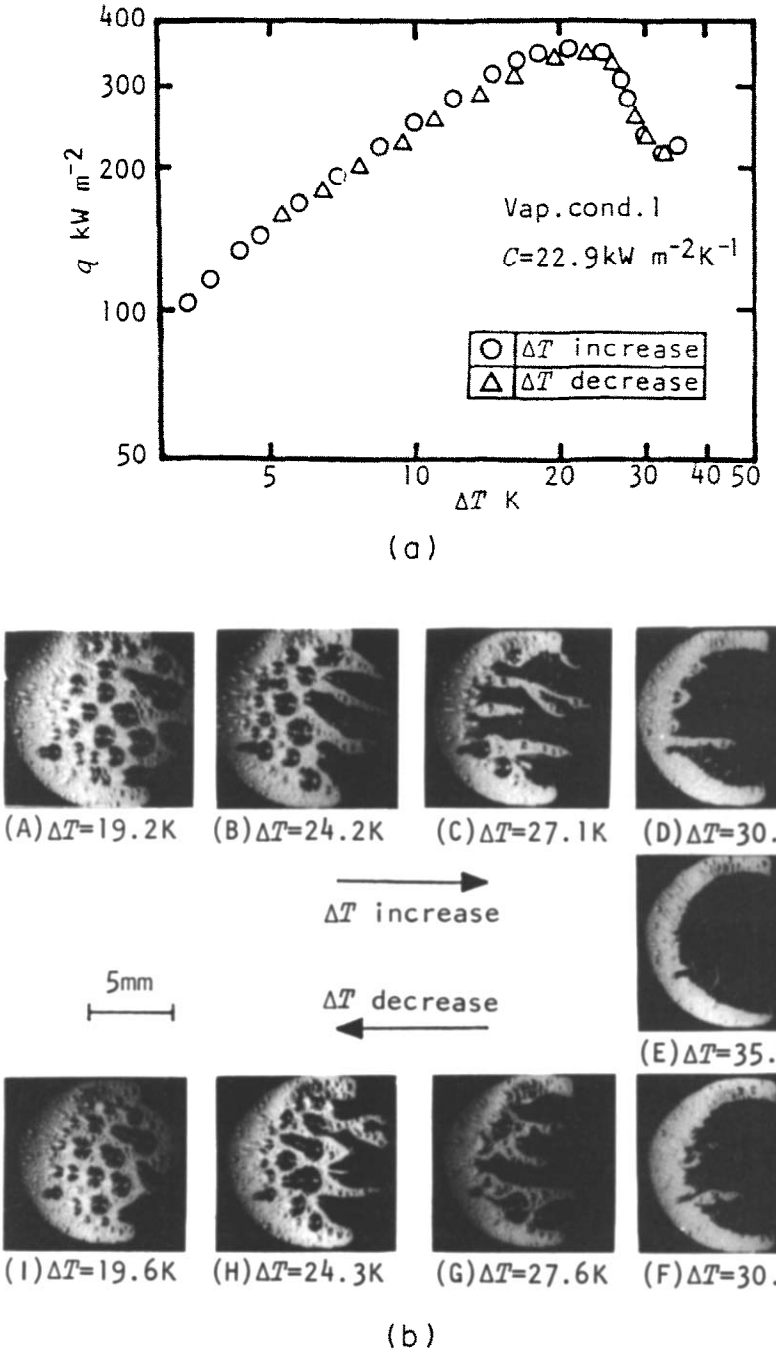

FIG. 10. Results using heat transfer surface III under vapor condition 1: (a) condensation curve; (b) aspects of condensation.

metrical and irreversible changes (Figs. 9(a) and (b)) when using a partially non-wettable edge at a relatively high vapor velocity. It was also the same for the curves using a wettable edge. Those results indicate that the reversibility of the condensation curve and the reversibility of the aspect of condensation have one-to-one correspondence.

The recovery from film to dropwise condensation was closely related to the state of the condensate rivulets formed during the shift from dropwise to film condensation. When the vapor force was relatively large, a large number of rivulets were formed during the process of increasing subcooling; the aspect of condensation shifted toward the film mode with the growth and the coalescence of these rivulets. Under a large vapor force for a partially non-wettable edge as shown in Figs. 9(a) and (b), the film mode could not return reversibly to dropwise mode of existing thin rivulets at the edge not connected with the non-wettable area during decreasing subcooling. Hence, the

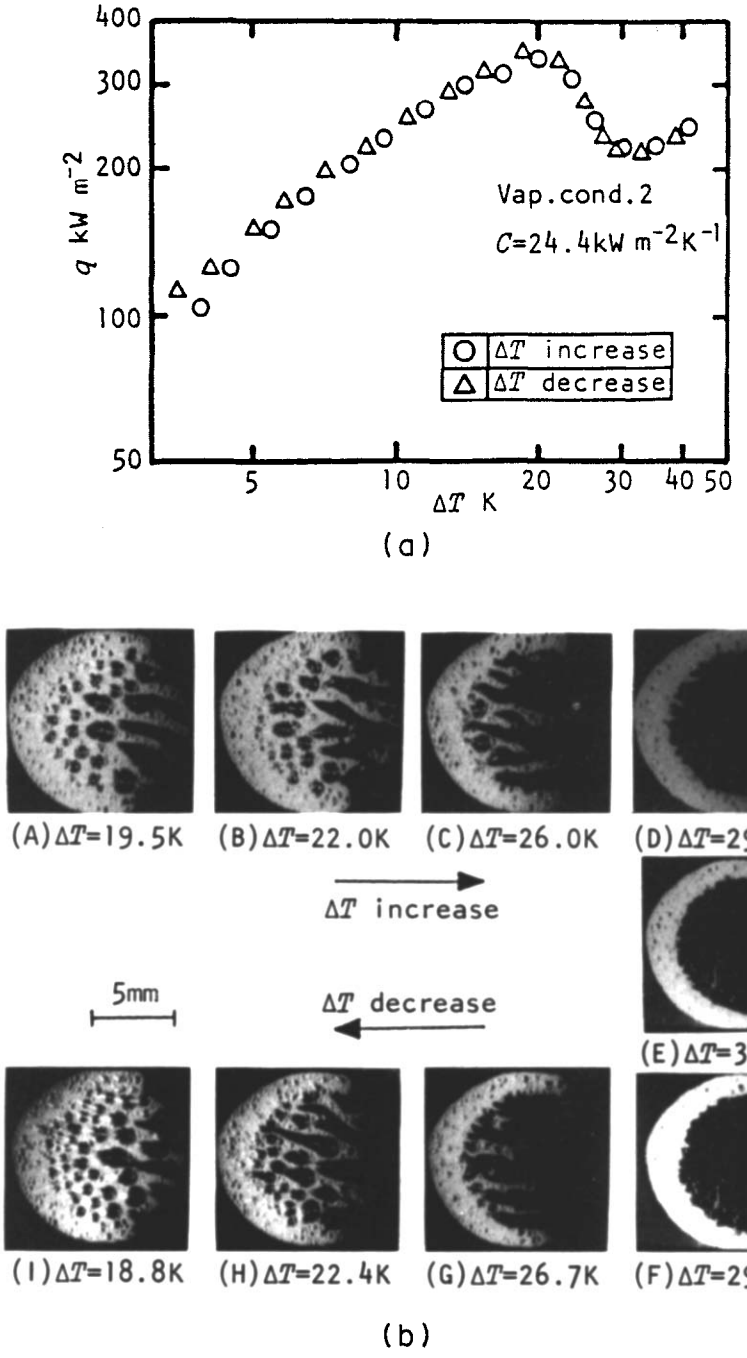

FIG. 11. Results using heat transfer surface III under vapor condition 2: (a) condensation curve; (b) aspects of condensation.

film condensation lasted until the liquid film began to break at the periphery not connected to the non-wettable edge. Contrary to this, under small vapor force, only a few rivulets were formed and the effect of the thin non-wettable edge was very large; the reversible curves could be obtained as shown in Figs. 8(a) and (b). For heat transfer surface III, the long non-wettable area enabled smooth returning to the state of existing rivulets of condensate; the reversible shifts were achieved independently of the number of rivulets (the magnitude of vapor force).

Table 2 shows the surface subcoolings and the heat fluxes at MHF points. All of these are experimental results using heat transfer surfaces II and III both for the processes of increasing and decreasing subcoolings and both for the transition of continuous and jump modes in the process of increasing subcooling. From comparison of the results for surface II under vapor

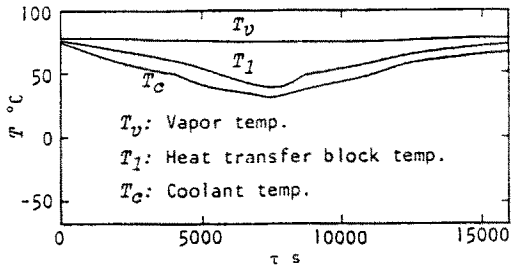

FIG. 12. Quasi-steady temperature variation.

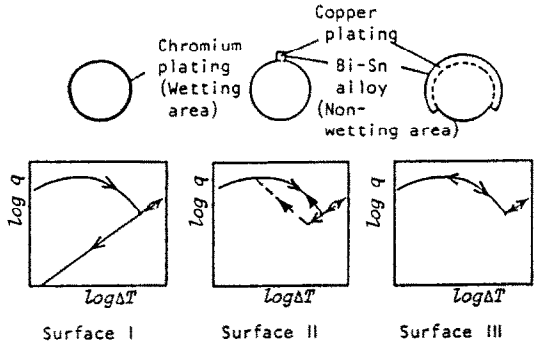

FIG. 13. Summary of transition modes. (Continuous modes in increasing subcooling processes. For heat transfer surface II, → shows the different cases depending on the vapor force.)

condition 1 and for surface III, the MHF points of the processes of decreasing subcooling are seen to be fixed for each vapor condition independently of the transition modes. In those cases of the continuous transition in increasing subcooling, the MHF points of increasing and decreasing surface subcoolings also coincided. However, they did not for surface II under vapor condition 2. Those results indicate that the MHF point for the process of decreasing subcooling was determined by the break condition of the condensate film independently of the instability of the overall heat transfer system.

5. CONCLUSIONS

The reversibility and the hysteresis of the condensation curves were investigated experimentally by using propylene glycol as a test vapor and the lyophobic surfaces having different edge conditions of wettability. The following conclusions were obtained.

(1) When the overall cooling-side conductance was large enough to obtain the continuous curve during the process of increasing subcooling, the edge conditions and also the vapor force were the controlling factors in determining the transition mode from film to dropwise condensation. The criterion to obtain the reversible curve was to achieve the reversible change of

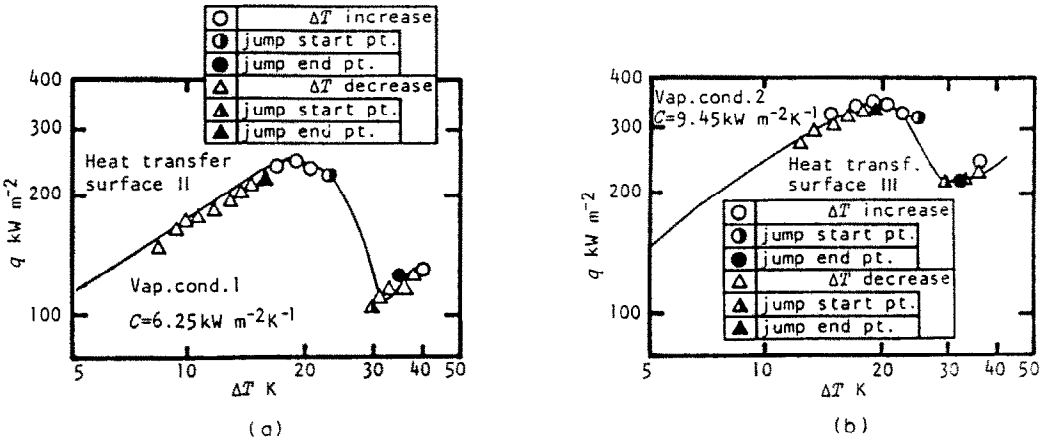

FIG. 14. Transition of jump mode (condensation curve): (a) heat transfer surface II, vapor condition 1; (b) heat transfer surface III, vapor condition 2.

Table 2. Comparison of surface subcoolings and heat fluxes at minimum heat flux points

Shift mode (ΔT increase)	Variation of ΔT	Heat transfer surface II				Heat transfer surface III				Overall cooling-side conductance, C (kW m⁻² K⁻¹)
		Vapor condition 1		Vapor condition 2		Vapor condition 1		Vapor condition 2		
		ΔT_{min} (K)	q_{min} (kW m^{-2})	ΔT_{min} (K)	q_{min} (kW m^{-2})	ΔT_{min} (K)	q_{min} (kW m^{-2})	ΔT_{min} (K)	q_{min} (kW m^{-2})	
Continuous	Increase	30.0	110	22.0	130	31.5	215	29.5	205	23 ~ 28
	Decrease	30.5	115	16.0	115	32.0	210	28.5	210	
Jump	Increase	32.5	130	29.0	135	32.0	210	31.0	210	5.7 ~ 10
	Decrease	29.5	110	20.5	120	30.0	210	28.5	205	

the aspect of condensation by making a non-wettable edge. Relatively long or many non-wettable edges were needed for a larger vapor force.

(2) The jump transition due to the instability of the overall heat transfer system with small overall cooling-side conductance brought about the hysteresis loop.

REFERENCES

1. T. Takeyama and S. Shimizu, On the transition of dropwise-film condensation, *Proc. Fifth Int. Heat Transfer Conf.*, Vol. 3, p. 274 (1974).
2. I. Tanasawa and Y. Utaka, Measurement of condensation curves for dropwise condensation of steam at atmospheric pressure, *Trans. ASME, J. Heat Transfer* **105**(3), 633 (1983).
3. M. Izumi, U. Susuki and T. Takeyama, Two hysteresis loops and effect of non-condensable gas in condensation curves, *Trans. Jap. Soc. Mech. Engng* **50**(454), 1600 (1984).
4. R. Wilmshurst and J. W. Rose, Dropwise and filmwise condensation of aniline, ethanediol and nitrobenzene, *Proc. Fifth Int. Heat Transfer Conf.*, Vol. 3, p. 269 (1974).
5. S. A. Stylianou and J. W. Rose, Drop-to-filmwise condensation transition (heat transfer measurements for ethanediol), *Int. J. Heat Mass Transfer* **26**, 747 (1983).
6. Y. Utaka, A. Saito, T. Tani, H. Shibuya and K. Katayama, Study on dropwise condensation curves (measurement of propylene glycol vapor on PTFE coated surface), *Bull. JSME* **28**(240), 1150 (1985).
7. Y. Utaka, A. Saito, H. Ishikawa and H. Yanagida, Study on dropwise condensation curves (dropwise to filmwise transition of propylene glycol, ethylene glycol and glycerol vapors on a copper surface using a monolayer type promoter (Part 1)), *Bull. JSME* **29**(258), 4228 (1986).
8. Y. Utaka, A. Saito and H. Yanagida, On the mechanism determining the transition mode from dropwise to film condensation, *Int. J. Heat Mass Transfer* **31**, 1113 (1988).

UNE ETUDE EXPERIMENTALE DE LA REVERSIBILITE ET DE L'HYSTERESIS DES COURBES DE CONDENSATION

Résumé—On présente une étude expérimentale des caractéristiques de transition concernant la réversibilité et la boucle d'hysteresis de la courbe de condensation. A partir des expériences avec la vapeur de propylène glycol sur des surfaces lyophobiques ayant trois conditions de bord de mouillabilité totale, mouillabilité partielle et non mouillabilité, on prouve que les modes de transition sont fortement affectés par ces conditions. On obtient la courbe réversible et/ou l'hysteresis. Les modes de transition pendant le sous-refroidissement décroissant sont étroitement liés aux aspects de la condensation dans des sous-refroidissements croissants. Bien que les modes pour le sous-refroidissement croissant soient déterminés par l'instabilité du système global de transfert thermique, ils sont fortement influencés par les conditions de bord et la vapeur. Pour une faible conductance globale qui joue sur le mode de saut, les boucles d'hysteresis apparaissent dans tout les cas.

EXPERIMENTELLE UNTERSUCHUNG ÜBER DIE REVERSIBILITÄT UND HYSTERESE DER KONDENSATIONSKURVEN

Zusammenfassung—Das Übergangansverhalten bei der Reversibilität und der Hysterese wird in einer experimentallen Studie untersucht. Die Ergebnisse der Kondensationsexperimente mit Propylenglykoldampf auf lyophoben Oberflächen mit drei unterschiedlichen Benetzungscharakteristiken (benetzbar, teilweise benetzbar, nicht benetzbar) haben gezeigt, daß das Übergangsverhalten stark von diesen Bedingungen beeinflußt wird. Unter der Bedingung großer kühlseitiger Gesamtleitfähigkeit, die zu einer stetigen Kurve bei steigender Oberflächenunterkühlungführt, erhält man reversible und/oder Hysteresekurven. Das Übergangsverhalten bei abnehmender Unterkühlung ist eng mit den Erscheinungen bei der Kondensation mit zunehmender Unterkühlung verknüpft. Obgleich das unterschiedliche Verhalten bei steigender Unterkühlung durch die Instabilität des gesamten wärmeübertragenden Systems bestimmt wird, besteht ebenfalls ein starker Einfluß der Randbedingungen und der Dampfströmung. Im Falle kleiner kühlseitiger Gesamtleitfähigkeit, die ein Sprungverhalten verursacht, treten in allen Fällen Hysteresesschleifen auf.

ЭКСПЕРИМЕНТАЛЬНОЕ ИССЛЕДОВАНИЕ ОБРАТИМОСТИ И ГИСТЕРЕЗИСА КРИВЫХ КОНДЕНСАЦИИ

Аннотация—экспериментально исследуются переходные характеристики обратимости и петли гистерезиса кривой конденсации. На основе результатов экспериментов по конденсации пропилен-гликолевого пара на лиофобных поверхностях при трех различных граничных условиях со смачиваемыми, частично смачиваемыми и несмачиваемыми поверхностями доказано, что данные условия оказывают сильное влияние на переходные режимы. Получены кривые обратимости и/или гистерезиса при большой общей теплопроводности охлаждающей поверхности, которая при увеличении недогрева поверхности описывается непрерывной кривой. Переходные режимы при уменьшении недогрева очень сходны с процессами конденсации в случае увеличения недогрева. Несмотря на то, что режимы увеличения недогрева определяются нестабильностью общего теплопереноса системы, большое воздействие на них оказывают граничные условия и давление пара. При малой общей теплопроводности охлаждающей поверхности, обусловливающей переходный режим, во всех случаях появляются петли гистерезиса.